Soft magnons in anisotropic ferromagnets

Bauer, G. E.W.; Tang, P.; Elyasi, M.; Blanter, Y. M.; Van Wees, B. J.

DOI
10.1103/PhysRevB.108.064431

Publication date
2023

Document Version
Final published version

Published in
Physical Review B

Soft magnons in anisotropic ferromagnets

G. E. W. Bauer,[1,2,3] P. Tang,[1] M. Elyasi,[1] Y. M. Blanter,[4] and B. J. van Wees[5]
[1] *WPI Advanced Institute for Materials Research, Tohoku University, 2-1-1, Katahira, Sendai 980-8577, Japan*
[2] *Institute for Materials Research and CSIS, Tohoku University, 2-1-1 Katahira, Sendai 980-8577, Japan*
[3] *Kavli Institute for Theoretical Sciences, University of the Chinese Academy of Sciences, Beijing 10090, China*
[4] *Kavli Institute of NanoScience, Delft University of Technology, 2628 CJ Delft, The Netherlands*
[5] *Physics of Nanodevices, Zernike Institute for Advanced Materials, University of Groningen, 9747 AG Groningen, The Netherlands*

(Received 20 April 2023; accepted 21 July 2023; published 28 August 2023)

We discuss spin-wave transport in anisotropic ferromagnets with an emphasis on the zeros of the band edges as a function of a magnetic field. An associated divergence of the magnon spin should be observable by enhanced magnon conductivities in nonlocal configurations, especially in two-dimensional ferromagnets.

DOI: 10.1103/PhysRevB.108.064431

I. INTRODUCTION

Magnonics is the study of the elementary excitations of the magnetic order, i.e., spin waves and their quanta called magnons. Several excellent textbooks cover the basic physics [1–3]. The field is believed to be competitive in future information, communication, and thermal management technologies [4,5].

In the exchange interaction-only continuum model the spin-wave dispersion is a parabola that shifts linearly with an applied magnetic field [1–3]. The gain of angular momentum of the ground state by flipping a single electron is $\hbar$. The associated change of the magnetic moment is $-2\mu_B$, where μ_B is the Bohr magneton. The exchange energy cost of a single spin flip is minimized by spreading this excitation over the whole system, forming a spin wave or its quantum, the magnon.

Magnetic dipolar interactions and spin-orbit interactions strongly affect the spin-wave dispersion of ferromagnets. Crystal anisotropies are the main consequence of the latter, and cause, for example, magnon gaps in the absence of an applied magnetic field. Only quite recently have researchers realized that the magnon spin is not a universal constant. Ando *et al.* [6] reported enhanced spin pumping by an elliptic magnetization precession, which, as we show below, can be interpreted as an enhanced magnon spin. Flebus *et al.* [7] reported that the exchange magnon polaron, i.e., the hybrid state of a magnon and a phonon, carries a spin between 0 and $\hbar$. Kamra and Belzig [8] predict super-Poissonian shot noise in the spin pumping from ferromagnets into metallic contacts based on a magnon spin that is enhanced from its standard value of $\hbar$ by anisotropy squeezing. These authors start from a lattice quantum spin Hamiltonian with local and magnetodipolar anisotropies and predicted magnon spins of around $4\hbar$ for the fundamental (Kittel) mode of an iron film. Kamra *et al.* [9] address the emergence of the magnon spins in antiferromagnets at weak applied magnetic fields. Neumann *et al.* [10] introduced an orbital contribution to the magnon magnetic moment. Yuan *et al.* [11] review the history of the magnon spin concept and its enhancement by quantum squeezing.

Magnon currents can be injected into ferromagnetic insulators by heavy-metal contacts, electrically by means of the spin Hall effect or by thermal gradients (spin Seebeck effect). Viceversa, magnons can pump a spin current into a heavy-metal contact and be detected by an inverse-spin-Hall voltage. Both effects may be combined to study magnon transport in magnetic insulators [12]. Films of ferrimagnetic yttrium iron garnet are well suited for magnon transport studies and can be grown with high quality down to a few monolayers [13]. The same technique also works well for antiferromagnetic hematite [14–16].

De Wal *et al.* [17] studied nonlocal magnon transport in an antiferromagnetic van der Waals film with a perpendicular Néel vector. An in-plane magnetic field cants the two sublattices until the material becomes ferrimagnetically ordered at the spin-flip transition, not unlike the in-plane spin texture of hematite at high fields. In the absence of additional anisotropies, the band gap of the spin-wave dispersion vanishes at this point, i.e., the magnons become soft. In contrast, our work focuses on the interpretation of soft magnons in terms of an effective magnon spin, the spin pumping by the magnetization dynamics, and the divergencies in the bulk magnon properties that dominate spin transport when the spin injection is efficient.

Here we make a step back by realizing that magnons can be soft in simple ferromagnets as well. Yuan and Duine already interpreted nonanalyticities in the magnon dispersion of anisotropic ferromagnets in terms of first- and second-order phase transitions [18], but do not address the magnon spin. We find that the magnon spin is strongly affected by the associated nonanalyticities of the dispersion relation and may even diverge. We illustrate the general concept of soft magnons and magnon spin for the three generic magnetic configurations in Fig. 1 in which applied magnetic fields and uniaxial anisotropies compete [18]. We predict observable enhancements of magnon transport in bulk materials in the

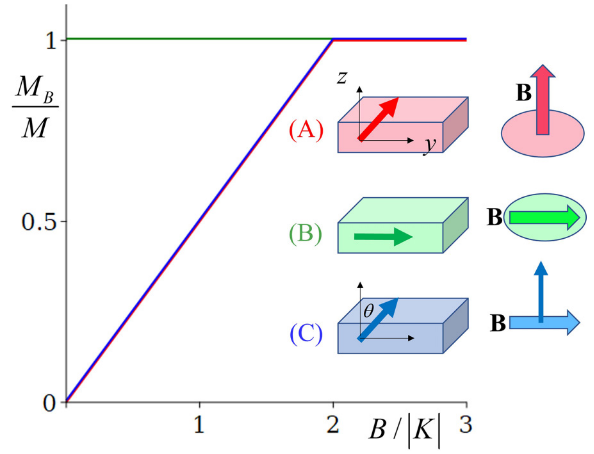

FIG. 1. Three configurations of ferromagnets with uniaxial magnetic anisotropies parameterized by K and magnetization M_B in the direction of the applied magnetic field B. Case (A) is an easy-plane ferromagnet with a magnetic field along z (red). In case (B) the field lies in the easy plane (green). In case (C) the field is normal to the easy z axis and θ is the tilt angle of the magnetization.

proximity of the soft magnon configurations. These results may partly explain the strong enhancement of the magnon transport at the spin-flip transition in antiferromagnets [19].

Sections II and III set the stage by rederiving results for the ground and low energy excitations in magnetic systems. In Sec. II we analyze the ground state by minimizing the classical magnetic free energy. We solve the linearized Landau-Lifshitz equations in Sec. III for the spin-wave dispersion relations, finding results that agree with those obtained from quantum spin models. In Sec. IV we address the magnon spin in a way we have not found in the literature. We show that the Hellman-Feynman theorem can be a useful tool to get hands on the magnon magnetic moment, but only when field and magnetization are collinear. In Sec. V we discuss possible experimental signatures of the large magnon spins close to the kinks in the magnon dispersion. Section VI contains a critical discussion of the model and recommendations for future work.

II. SPIN HAMILTONIANS AND FERROMAGNETIC GROUND STATES

We consider Hamiltonians for local spins $\hat{\mathbf{S}}_i$ and magnetic moments $\hat{\mathbf{M}}_i = -\gamma\hbar\hat{\mathbf{S}}_i$ on lattice sites i:

$$\mathcal{H} = \gamma\hbar\sum_i \hat{\mathbf{S}}_i\cdot\mathbf{B} - \sum_{ij} J_{ij}(\hat{\mathbf{S}}_i\cdot\hat{\mathbf{S}}_j) - \gamma\hbar\bar{K}\sum_i \left(\hat{S}_i^z\right)^2, \quad (1)$$

where J_{ij} is the exchange integral between spins on sites $i \neq j$, $-\gamma$ is the gyromagnetic ratio of an electron, and $\mathbf{B}$ is a constant external magnetic field. We focus here on $J_{ij} > 0$ that leads to ferromagnetic order. $\bar{K}$ is a uniaxial anisotropy field along the Cartesian z direction, and $\bar{K} > 0$ ($\bar{K} < 0$) corresponds to an easy-axis (easy-plane) ferromagnet.

The ground state that minimizes the total energy of the macroscopic system is ferromagnetic. The total spin of the system $\hat{\mathbf{S}} = \sum_i \hat{\mathbf{S}}_i$ then becomes a classical vector $\mathbf{S}$ corresponding to a magnetization density $\mathbf{M} = -(\gamma\hbar/\Omega)\mathbf{S}$, where Ω is the crystal volume. The associated energy density without irrelevant constant terms reads

$$E(\mathbf{M}) = -\mathbf{M}\cdot\mathbf{B} - \frac{\bar{K}}{M}(M_z)^2 + \frac{D}{2M}(\nabla\mathbf{M})^2, \quad (2)$$

where $M = |\mathbf{M}| = (\gamma\hbar S/\Omega)$ and $S = |\mathbf{S}|$. The spin-wave stiffness D represents the exchange energy cost of spatial deformations in the continuum limit that depends on crystal structure and the exchange parameters J_{ij}. We disregard dipolar and spin-orbit interactions that favor the formation of magnetic textures. The magnetizations of the ground states are then constant in space with zero exchange energy cost. The demagnetization energy in magnetic films with surface normal $\mathbf{n}$ along z can be absorbed into the anisotropy field $K = (S\bar{K})/(\gamma\hbar) + M$. We do encounter here here the hysteresis when cycling magnetic fields along an easy axis, as described by the Stoner-Wohlfarth model, see Ref. [2], p. 102.

We discuss here three configurations: (A) Easy xy-plane anisotropy ($K < 0$) and the magnetic field normal to the plane; (B) easy xy-plane anisotropy with an in-plane magnetic field (Kittel problem); and (C) easy z-axis anisotropy ($K > 0$) with a magnetic field in the y direction. Other configurations such as in-plane easy-axis, etc. give similar results. The parameters depend on temperature but may be treated as constants when temperatures are sufficiently below the phase transition.

We are interested in the nonanalyticities that emerge at critical fields $B_c = 0$ for case (B) and $B_c = 2|K|$ for A and B.

In case A, $\mathbf{B} = B\mathbf{z}$, where $\mathbf{z}$ is the unit vector along the anisotropy axis, the energy and magnetizations are nonanalytic at $B_c = 2|K|$

$$\frac{E_0^{(A)}}{M} = \begin{cases} -\frac{B^2}{4|K|} & \text{for } B < 2|K| \\ |K| - B & \phantom{\text{for }} B > 2|K| \end{cases} \quad (3)$$

$$\frac{M_z}{M} = \begin{cases} \frac{B}{2|K|} & \text{for } B < 2|K| \\ 1 & \phantom{\text{for }} B > 2|K|. \end{cases} \quad (4)$$

In case B, the energy as a function of the magnetic field B

$$E^{(B)}(\mathbf{M}) = -M_y B + \frac{|K|}{M}M_z^2 \quad (5)$$

is minimal for $\mathbf{M}_0 = (0, M, 0)$ for all $B \neq 0$. Finally, in C a field $\mathbf{B} = B\mathbf{y}$ along the y axis tilts the magnetization into the yz plane with $\mathbf{M}_0 = M(0, \sin\theta, \cos\theta)$, where θ is the angle with the out-of-plane direction. Eq. (2)

$$\frac{E^{(C)}(\theta)}{M} = -K\cos^2\theta - B\sin\theta \quad (6)$$

is minimized for

$$\sin\theta = \begin{cases} \frac{B}{2K} & \text{for } B < B_c \\ 1 & \phantom{\text{for }} B > B_c \end{cases}. \quad (7)$$

Above $B_c = 2K$, the field and magnetization are aligned.

III. SPIN-WAVE DISPERSION

Here we consider the frequency dispersion relation for the elementary excitations in homogeneous extended magnets that can be bulk crystals, thin films, or two-dimensional systems. The excitation frequencies are sharply defined in the

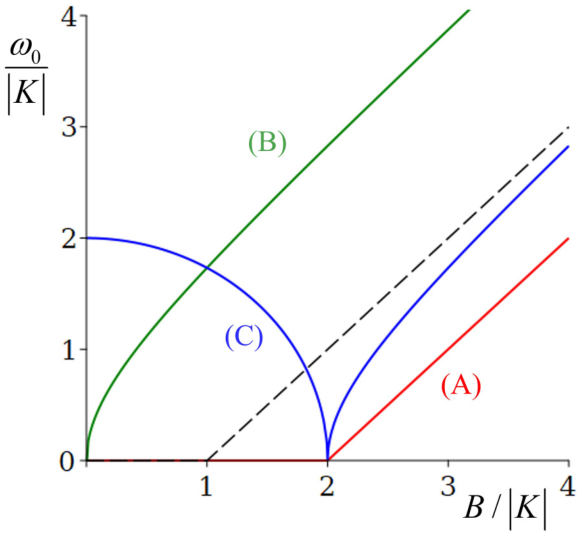

FIG. 2. Spin-wave frequency of the magnon band edges for the configurations (A)–(C) in Fig. 1. The dashed black line $\omega_0/\gamma = B - K$ is the asymptotic form of case (B) at large fields.

limit of small amplitude oscillations, in which spin waves can be mapped on a set of noninteracting harmonic oscillators. The magnon Hamiltonian is the lowest-order term in the Holstein-Primakoff expansion of the spin Hamiltonian, which can subsequently be diagonalized by a Bogoliubov transformation, see Ref. [1], p. 83, Ref. [2], p. 277, Ref. [18]).

Here we chose to start from the Landau-Lifshitz equation $\dot{\mathbf{M}} = -\gamma(\mathbf{M} \times \mathbf{B}_{\text{eff}})$, in which $\mathbf{B}_{\text{eff}} = -\partial E(\mathbf{M})/\partial \mathbf{M}$ and $E(\mathbf{M})$ is the classical magnetic free energy introduced above. Writing $\mathbf{M}_q = \mathbf{M}_0 + \mathbf{m}_q$ and $\mathbf{B}_{\text{eff}} = \mathbf{B} + \mathbf{b}_\mathbf{q}$ to leading order in the small transverse excitation amplitudes $\mathbf{m}_q \cdot \mathbf{M}_0 = 0$, the spin-wave frequencies ω_q for wave vector $\mathbf{q}$ are the solutions of

$$(i\omega_q - \gamma \mathbf{B}\times)\mathbf{m}_q = -\gamma \mathbf{M}_0 \times \mathbf{b}_q. \tag{8}$$

For simplicity, we compute ω_q without the dipolar interactions that cause well-known anisotropic corrections for $q \neq 0$, but do not affect the band edges in Fig. 2. The results agree with those obtained from the lowest-order Holstein-Primakov expansion of the corresponding spin Hamiltonians.

When the magnetic field is normal to the easy plane (A), the spin-wave dispersion reads

$$\omega_q^{(A)} = \gamma \begin{cases} \sqrt{Dq^2\left(2|K| - \frac{B^2}{2K^2} + Dq^2\right)} & \text{for } B < 2|K| \\ B - 2|K| + Dq^2 & \text{for } B > 2|K| \end{cases}. \tag{9}$$

The spin-wave frequency of the uniform precession ($q = 0$) vanishes for magnetic fields below B_c because the torques generated by the anisotropy and applied fields cancel. The energies for all magnetization directions that lie on a cone with opening angle θ are the same, so the ground state is highly degenerate.

The Kittel problem B leads to

$$\omega_q^{(B)} = \gamma\sqrt{(B + Dq^2 + 2K)(B + Dq^2)}. \tag{10}$$

The anisotropy qualitatively changes the dispersion at small magnetic fields from $\omega_0^{(B)} = \gamma B$ for $K = 0$ to $\omega_0^{(B)} \sim \gamma\sqrt{B}$ when $K > B$. The anisotropy breaks the axial symmetry and mixes the anticlockwise circular precession mode with positive frequencies and the forbidden clockwise one with negative frequencies, which leads to the square-root dependence rather than $2\gamma K$, the linearly extrapolated value from the high-field region.

In configuration C (as in A), magnetization and field are not collinear for fields $B < B_c$. By rotating the coordinate system around the x axis by θ such that $\mathbf{M}_0'$ is along z', we can impose the magnon approximation by solving for small amplitude oscillations $\mathbf{m}_q' \cdot \mathbf{M}_0' = 0$. The result is

$$\omega_q^{(C)} = \gamma \begin{cases} \sqrt{\frac{1}{2K}(2K + Dq^2)(4K^2 - B^2 + 2DKq^2)} \\ \sqrt{(B + Dq^2 - 2K)(B + Dq^2)} \end{cases} \text{for } \begin{matrix} B < 2|K| \\ B > 2|K| \end{matrix}. \tag{11}$$

We observe that the B dependence of the collinear configuration equals that of the Kittel mode shifted by $2|K|$ to higher magnetic fields.

IV. MAGNON SPIN AND HELLMANN-FEYNMAN THEOREM

An excited state $|q\rangle$ with energy $\varepsilon_q = \hbar\omega_q$ of an arbitrary spin Hamiltonian carries a spin magnetic moment $\boldsymbol{\mu}_q = \langle q|\hat{\mathbf{M}}|q\rangle - \mathbf{M}_0$, where $\hat{\mathbf{M}} = -\gamma\hbar\sum_i \hat{\mathbf{S}}_i$. Consider a spin system with zero-field Hamiltonian $\mathcal{H}_S$ that interacts with constant applied magnetic field $\mathbf{B}$ by the Zeeman interaction

$$\mathcal{H} = \mathcal{H}_S - \hat{\mathbf{M}} \cdot \mathbf{B}. \tag{12}$$

The Hellmann-Feynman theorem then states that for simplicity in the absence of textures,

$$\boldsymbol{\mu}_q = -\frac{\partial \varepsilon_q}{\partial B_\parallel}\frac{\mathbf{M_0}}{M}, \tag{13}$$

where $B_\parallel = \mathbf{B} \cdot \mathbf{M}_0/M$. For our classical spin system, we replace ε_q with $\Delta E_q = E(\mathbf{M}_0 + \boldsymbol{\mu}_q) - E(\mathbf{M}_0)$. When the magnetization and the applied field are parallel, we can simply read off the spin of the excited state from the magnon spectrum as a function of the applied field. When $\mathbf{M} \nparallel \mathbf{B}$, the situation is more complicated and the Hellmann-Feynman theorem requires additional calculations. Configurations A and C at fields $B < 2K$, for example, acquire an orbital correction [10]

$$\mu_q = -\frac{d\varepsilon_q}{dB} + \frac{\partial \varepsilon_q}{\partial \theta}\frac{\partial \theta}{\partial B}, \tag{14}$$

where θ is the equilibrium tilt angle. The implicit dependence on the field enters here with an opposite sign compared to Ref. [10].

To leading order, the solutions of the LL equation are transverse, i.e., $\mathbf{m}_q \cdot \mathbf{M}_0 = O(m_q^2)$. If we transform back into the time domain, the transverse components oscillate with the spin-wave frequency and average out to zero. A magnon moment along the magnetization direction persists in the time average as

$$\frac{\mu_q}{2\mu_B} \approx -\frac{|\mathbf{m}_q|^2}{2M}\frac{\mathbf{M}_0}{M}. \tag{15}$$

The amplitudes of the solutions of the LL equation are continuous but can be quantized by requiring that the minimum excitation energy of a mode with energy ε_q is discrete:

$$\Delta E_q = E(\mathbf{M}_q) - E_0 = \hbar\omega_q. \tag{16}$$

By normalizing the mode amplitudes in this way we can compute the spin of a single magnon for our three configurations A–C.

In case A, the moment of a single magnon $\mu_q^{(A)} = -2\mu_B$ for $B > B_c$ follows from the Hellmann-Feynman theorem. Spin and magnetization are not collinear for $B < B_c$. The LL equation then leads to a magnon magnetic moment along the equilibrium magnetization direction of

$$\frac{\mu_q^{(A)}}{2\mu_B} = -\frac{|K| - \frac{B^2}{4|K|} + Dq^2}{\sqrt{Dq^2\left(2|K| - \frac{B^2}{2|K|} + Dq^2\right)}} \tag{17}$$

that diverges when $q \to 0$ because the degeneracy of all magnetization directions on the cone with angle θ allows coherent precession of the magnetization without an energy cost.

In case B, we can compute the magnon spin simply as a derivative of the frequency with respect to the applied magnetic field from the Hellmann-Feynman theorem Eq. (13) since $\mathbf{B} \parallel \mathbf{M}$:

$$\frac{\mu_q^{(B)}}{2\mu_B} = -\frac{B + K + Dq^2}{\sqrt{(B + Dq^2 + 2K)(B + Dq^2)}}. \tag{18}$$

In the zero field limit, $\mu_0^{(B)} = -2\mu_B/\sqrt{K/(2B)}$ diverges. The anisotropy mixes right and left precession modes to create an elliptic motion that in the limit of zero magnetic field leads to a linear x-polarized motion in the easy plane. As in case A the restoring torque vanishes in this limit, which allows the magnon amplitude to become large.

Also in the high-field regime $B > B_c$ of the case C, we can use the Hellmann-Feynman theorem without having to worry about orbital terms

$$\frac{\mu_q^{(C)}}{2\mu_B} = -\frac{(B + Dq^2) + (B + Dq^2 - 2K)}{\sqrt{(B + Dq^2 - 2K)(B + Dq^2)}} \quad \text{for } B > B_c, \tag{19}$$

which is a shifted version of $\mu_q^{(B)}$. $\mu_0^{(C)}$ diverges for $B \downarrow B_c$ at the band edge q = 0 like $1/\sqrt{B - B_c}$ because the torque in the out-of-plane z direction vanishes. The magnon spin for the canted configuration ($B < B_c$) can be computed directly from the solutions of the LL equation. Along the canted equilibrium magnetization direction

$$\frac{\mu_q^{(C)}}{2\mu_B} = -\frac{\sqrt{Dq^2 + 2K}}{\sqrt{2K}} \times \frac{\sqrt{4K^2 - B^2 + 2DKq^2}(8K^2 - B^2 + 4DKq^2)}{(4K^2 - B^2)4K + (16K^2 + 4KDq^2 - 3B^2)Dq^2}. \tag{20}$$

which shows a square root divergence when $B \uparrow B_c$. In Fig. 3 we plot the in-plane projection of the magnon spin at the band edges along the y direction, i.e., the spin component $\mu_0^{(C)} \sin\theta$ that can be injected and detected by Pt contacts, as well as the z component along the easy axis.

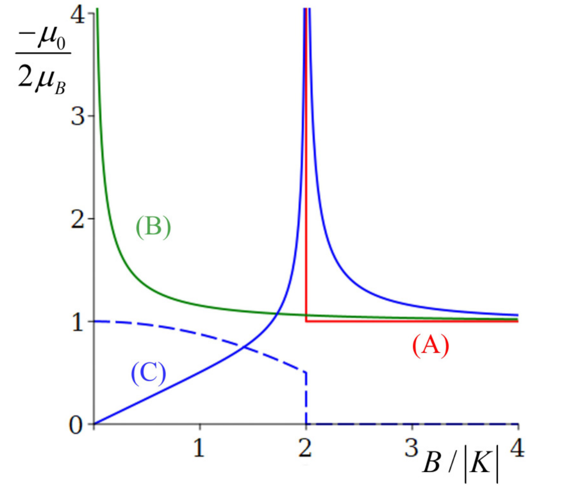

FIG. 3. Magnon spin at the band edges for the configurations (A)–(C) in Fig. 1. In (C) the magnon spin is tilted for $B < 2|K|$ with a component in the y (full curve) and z directions (dashed curve).

V. TRANSPORT

We now discuss some physical consequences of the results derived above. In case A the magnons are gapless up to $B_c = 2|K|$. The absence of an energy cost of the in-plane magnetization amplitude implies that the equilibrium direction is arbitrary and depends on the history, remaining in-plane anisotropies, or disorder. Even small energy gains of the magnetodipolar interactions break a uniform magnetization down into domains. At B_c the magnon spin jumps to its standard value of $-2\mu_B$. In case B interesting effects may occur when the magnon spin diverges at vanishing magnetic fields but it is again difficult to control the equilibrium magnetic order. Therefore, the soft magnon in the field dependence of case C at the critical field looks most interesting. While the fluctuations and the associated magnon spin become large, the finite applied field hinders the breaking of the magnetic order even when the magnon gap vanishes. Hence, we focus on case C with an applied magnetic field that approaches the critical value from above. We address magnon transport in bulk materials and in two-dimensional ferromagnets.

A. Spin pumping

The magnon spin affects the spin pumping [6] and spin pumping shot noise [8]. The spin pumped into the metal by the dynamics of an insulating or metallic ferromagnet in units of ampere reads

$$\mathbf{J}_s = \frac{e}{2\pi}\left[\frac{g_r}{M_0^2}\mathbf{M} \times \dot{\mathbf{M}} + \frac{g_i}{M_0}\dot{\mathbf{M}}\right], \tag{21}$$

where $g_r + ig_i$ is the dimensionless interface spin-mixing conductance [20]. Inserting the LL equation for case C and $B \downarrow B_c$

leads to a dc spin current:

$$J_s^{(\mathrm{dc})} = \frac{eg_r}{2\pi}\frac{2\mu_B N}{M_0}\omega_0, \tag{22}$$

where N is the number of magnons in the Kittel mode. The vanishing resonance frequency of soft magnons cancels the divergence in the magnon spin.

B. Magnon conductivity and spin Seebeck effect

Next, we consider diffuse dc magnon transport in a bulk ferromagnet under gradients of temperature or magnon chemical potential with a special focus on the magnon conductivity in configuration C. We disregard the spin injection by Pt contact, which is allowed when transport is limited by the magnon propagation in the bulk of the ferromagnet. Yuan and Duine address the opposite limit of interface-dominated magnon transport that is also enhanced but not affected by the nonanalyticities in the magnon spin [18].

We employ the relaxation time approximation to the steady-state linearized Boltzmann equation for the distribution function $f(\mathbf{q},\mathbf{r};t)$

$$\frac{\partial f(\mathbf{q},\mathbf{r};t)}{\partial t} + \mathbf{v}_\mathbf{q}\cdot\nabla f(\mathbf{q},\mathbf{r};t) = \left(\frac{\partial f}{\partial t}\right)_{\mathrm{col}}, \tag{23}$$

where $\mathbf{v}_\mathbf{q} = \partial\omega_\mathbf{q}/\partial\mathbf{q}$ is the group velocity. In the steady state $\partial_t f = 0$. In the constant relaxation time (τ_r) approximation the collision term $(\partial_t f)_{\mathrm{col}} = -(f - f_0)/\tau_r^{(nd)}$ and $f_0 = [\exp(\frac{\hbar\omega_\mathbf{q}}{kT}) - 1]^{-1}$ is the Planck distribution. $\tau_r^{(nd)}$ parameterizes the scattering of magnons at magnetic disorder, phonons, and other magnons. It may depend strongly on temperature and frequency and be very different for $n = 2, 3$ dimensions [13]. The magnon current is polarized along the equilibrium magnetization $\mathbf{M}_0$. We disregard the magnetodipolar interactions on the dispersion relation since these cancel to a large extent in magnon transport except at very low temperatures. We are interested in the magnon conductivity $\sigma_m^{(nd)}$ (spin Seebeck coefficient $S_m^{(nd)}$) that characterizes the magnon spin current under a gradient in the magnon chemical potential (temperature). In electric units $[\sigma_m^{(nd)}] = \mathrm{Sm}^{2-n}$ and $[S_m^{(nd)}] = \mathrm{V/m}$ [13]:

$$\sigma_m^{(nd)} = \frac{e^2\tau_r^{(nd)}}{k_B T}\int\frac{dq^n}{(2\pi)^n}\frac{-\mu_q}{2\mu_B}v_q^2 f_0^2 e^{\frac{\hbar\omega_\mathbf{q}}{k_B T}}, \tag{24}$$

$$\sigma_m^{(nd)} S_m^{(nd)} = \frac{e\tau_r^{(nd)}}{k_B T^2}\int\frac{dq^n}{(2\pi)^n}\frac{-\mu_q}{2\mu_B}\hbar\omega_q v_q^2 f_0^2 e^{\frac{\hbar\omega_\mathbf{q}}{k_B T}}, \tag{25}$$

where $v_q = \partial\omega_q/\partial k_y$ is the group velocity in the transport y direction. Typical frequencies are in the GHz regime, so assuming that temperatures are not too low, $k_B T \gg \hbar\omega_q$. The combination $\mu_q\omega_q$ in the integrand of the spin Seebeck coefficient is analytic when the magnon turns soft. So we do not expect anomalies in thermally driven spin transport.

An artifact of the above equations, derived for a continuum model of the lattice, the constant relaxation time approximation, and the high-temperature limit, is the divergence of Eq. (24) at high wave numbers. When $K = 0$ and in three dimensions this can be regulated by

$$\sigma_m^{(3d)} = \frac{e^2}{\hbar^2}\frac{2}{3\pi^2}\tau_r^{(3d)}k_B T \times\left(Q_\infty + \frac{Bq}{2(DQ_\infty^2 + B)} - \frac{3}{2}\sqrt{\frac{B}{D}}\arctan\left(\sqrt{\frac{D}{B}}Q_\infty\right)\right), \tag{26}$$

where Q_∞ is an ultraviolet cutoff, at room temperature provided by the onset of strong magnon-phonon scattering at THz frequencies. Including the easy axis anisotropy $K > 0$ causes a logarithmic divergence at the critical field $B \downarrow B_c$. We avoid it by a low-momentum cutoff Q_0 that can be rationalized by a residual in-plane anisotropy or disorder. To leading orders for large Q_∞ and small Q_0^2 :

$$\sigma_m^{(3d)} \to \frac{e^2}{\hbar^2}\frac{2}{3\pi^2}\tau_r^{(3d)}k_B T\left(Q_\infty - \frac{\sqrt{2}}{16}\sqrt{\frac{K}{D}}\ln\frac{DQ_0^2}{8K}\right). \tag{27}$$

The last term is the conductivity enhancement by the soft mode magnon.

In two dimensions and $K = 0$

$$\sigma_m^{(2d)} = \frac{e^2}{\hbar^2}\frac{1}{\pi}\tau_r^{(2d)}k_B T e^2\tau_r^{(2d)}\frac{k_B T}{\pi}\frac{1}{2} \times\left[\ln\left(1 + \frac{DQ_\infty^2}{B}\right) + \frac{B}{B + DQ_\infty^2}\right] \tag{28}$$

the divergence is logarithmic but with a vanishing magnon gap $B \to 0$ there is now also a logarithmic infrared divergence for constant magnon spin, which is caused by the discontinuous magnonic density of states at the band edge. Including the divergent magnon spin when $K > 0$, to leading order in a small Q_0 and large Q_∞, and for $B \downarrow B_c$

$$\sigma_m^{(2d)} \to e^2\tau_r^{(2d)}\frac{k_B T}{\pi}\left[\ln\left(\sqrt{\frac{2D}{K}}Q_\infty\right) + \sqrt{\frac{K}{2D}}\frac{1}{4Q_0}\right] \tag{29}$$

The high-momentum divergence is still logarithmic, but the low-momentum one becomes algebraic. This implies a dimensionally enhanced magnon transport around the critical magnetic field in van der Waals ferromagnets with perpendicular magnetization that as discussed below, should be experimentally observable.

VI. DISCUSSION

Several processes regulate the enhanced fluctuations that cause the divergence of the magnon spin reported here, but should not destroy the predicted enhancement of spin pumping and spin transport. The situation is reminiscent of the singular compensation points in the phase diagrams of collinear ferrimagnets. These points occur when the angular momentum or magnetization of the magnetic sublattices cancel each other out, resulting in, e.g., enhanced domain wall velocities in their vicinity [21].

The magnon spin of the Kittel mode can be observed by spin pumping under ferromagnetic resonance. Ando *et al.* [6] indeed reported that the ellipticity of the magnetization precession under ferromagnetic resonance conditions increases the spin pumping, a finding that we interpret as evidence for an enhanced magnon spin. However, the resonance frequency also enters the pumped spin current, and the product spin×frequency remains well behaved for soft magnons. Similarly, the integrand for the spin Seebeck coefficient (25) does not diverge.

Magnon transport in electric insulators can be measured by heavy-metal contacts that serve as spin injectors and detectors. The magnon conductivities are accessible when the injector and detector distance does not exceed the magnon diffusion length, which requires high magnetic quality. YIG films can be tuned to a perpendicular magnetization by doping and epitaxial strain [22]. The hexagonal barium ferrite ($BaFe_{12}O_{19}$) has a perpendicular anisotropy field of 1.7 teslas and damping constant $\alpha = 10^{-3}$ [23]. Other options are electrically insulating van der Waals ferromagnets with perpendicular magnetization such as CrI_3 [24]. With minor adaptions, the present formalism can be used as well for magnetic films (strips) with an in-plane easy crystal (demagnetization) anisotropy axis and an in-plane magnetic field applied at right angles to it.

We estimate the magnitude of the expected effects from Eqs. (27), (29) by adopting the spin-wave stiffness of YIG $D = 5 \cdot 10^{-17}\,\mathrm{Tm}^2$, a perpendicular anisotropy $K = 1\,\mathrm{T}$, a high-momentum cutoff frequency of 1 THz, and an in-plane anisotropy of 1 mT. This leads to an enhancement of the magnon conductivity at the soft magnon point of ∼2 for three-dimensional and ∼5 for two-dimensional magnets.

The divergences reported here occur only in materials with weak residual anisotropies, i.e., a sufficiently small cutoff Q_0. Moreover, nonparabolicities render the magnon approximation invalid when the spin-wave amplitudes become large by large magnon spins and/or numbers. The implied magnon interactions may act as a brake on the dynamics. The predicted numbers at the critical points should therefore be taken with a grain of salt, but the enhancement of the magnon thermal conductivity close to the softening of the magnon modes should persist even when these factors are taken into account.

VII. CONCLUSIONS

We considered the spin waves of ferromagnetic magnons as a function of an applied magnetic field, focusing on the singular points at which the band edges (nearly) vanish. The more general conclusions such as the relation between the Hellmann-Feynman theorem for collinear systems also hold for antiferromagnets. We predict enhanced nonlocal magnon transport caused by the divergence of the magnon spin for magnets with a magnetic field applied perpendicular to a uniaxial magnetic anisotropy, which is stronger in two than in three dimensions. The effect should contribute to the observation of magnon transport above and down to the spin-flip transition at which the spin sublattices are forced to align ferromagnetically [17] and we expect enhanced nonlocal signals carried by the soft acoustic magnon as in case C. However, more work is necessary to fully understand the experiments [19].

The present calculations of the transport properties address the linear response at elevated temperatures, disregarding the effect of nonlinear terms that are likely to become important. Higher harmonic generation is easier for floppy magnetic order but is at vanishing applied fields complicated by spontaneous magnetic textures [25,26], which may not interfere when the soft magnon is shifted to sufficiently large magnetic fields. It should also be interesting to study the nonlinearities of propagating soft magnons by microwave spectroscopy [27].

ACKNOWLEDGMENTS

P.T. and G.B. acknowledge the financial support by JSPS KAKENHI Grants No. 19H00645 and No. 22H04965. B.W. was supported by the European Union's Horizon 2020 program under Grant Agreement No. 785219 and 881603, the NWO Spinoza prize, and ERC Advanced Grant 2DMAGSPIN (Grant Agreement No. 101053054). We thank A. Kamra for his comments on the manuscript and Huaiyang Yuan for alerting us to Ref. [18].

[1] A. G. Gurevich and G. A. Melkov, *Magnetization Oscillations and Waves* (CRC Press, London, 1996).

[2] D. D. Stancil and A. Prabhakar, *Spin Waves* (Springer, New York, 2009).

[3] S. M. Rezende, *Fundamentals of Magnonics* (Springer, Cham, 2020).

[4] A. Barman *et al.*, The 2021 magnonics roadmap, J. Phys.: Condens. Matter **33**, 413001 (2021).

[5] A. V. Chumak *et al.*, Advances in magnetics: roadmap on spin-wave computing, IEEE Trans. Magn. **58**, 1 (2022).

[6] K. Ando, S. Takahashi, J. Ieda, Y. Kajiwara, H. Nakayama, T. Yoshino, K. Harii, Y. Fujikawa, M. Matsuo, S. Maekawa, and E. Saitoh, Inverse spin-Hall effect induced by spin pumping in metallic system, J. Appl. Phys. **109**, 103913 (2011).

[7] B. Flebus, K. Shen, T. Kikkawa, K. Uchida, Z. Qiu, E. Saitoh, R. A. Duine, and G. E. W. Bauer, Magnon-polaron transport in magnetic insulators, Phys. Rev. B **95**, 144420 (2017).

[8] A. Kamra and W. Belzig, Super-Poissonian Shot Noise of Squeezed-Magnon Mediated Spin Transport, Phys. Rev. Lett. **116**, 146601 (2016).

[9] A. Kamra, U. Agrawal, and W. Belzig, Noninteger-spin magnonic excitations in untextured magnets, Phys. Rev. B **96**, 020411(R) (2017).

[10] R. R. Neumann, A. Mook, J. Henk, and I. Mertig, Orbital Magnetic Moment of Magnons, Phys. Rev. Lett. **125**, 117209 (2020).

[11] H. Y. Yuan, Y. Cao, A. Kamra, R. A. Duine, and P. Yan, Quantum magnonics: When magnon spintronics meets quantum information science, Phys. Rep. **965**, 1 (2022).

[12] L. J. Cornelissen, J. Liu, R. A. Duine, J. Ben Youssef, and B. J. van Wees, Long-distance transport of magnon spin information in a magnetic insulator at room temperature, Nature Phys. **11**, 1022 (2015).

[13] X.-Y. Wei, O. A. Santos, C. H. S. Lusero, G. E. W. Bauer, J. Ben Youssef, and B. J. van Wees, Giant magnon spin conductivity in ultrathin yttrium iron garnet films, Nat. Mat. **21**, 1352 (2022).
[14] R. Lebrun, A. Ross, S. A. Bender, A. Qaiumzadeh, L. Baldrati, J. Cramer, A. Brataas, R. A. Duine, and M. Kläui, Long-distance spin transport in a crystalline antiferromagnetic iron oxide, Nature (London) **561**, 222 (2018).
[15] T. Wimmer, A. Kamra, J. Gückelhorn, M. Opel, S. Geprägs, R. Gross, H. Huebl, and M. Althammer, Observation of Antiferromagnetic Magnon Pseudospin Dynamics and the Hanle Effect, Phys. Rev. Lett. **125**, 247204 (2020).
[16] J. Han, P. Zhang, Z. Bi *et al.*, Birefringence-like spin transport via linearly polarized antiferromagnetic magnons, Nat. Nanotech. **15**, 563 (2020).
[17] D. K. de Wal, A. Iwens, T. Liu, P. Tang, G. E. W. Bauer, and B. J. van Wees, Long distance magnon transport in the van der Waals antiferromagnet $CrPS_4$, Phys. Rev. B **107**, L180403 (2023).
[18] H. Y. Yuan and R. A. Duine, Universal field dependence of magnetic resonance near zero frequency, Phys. Rev. B **103**, 134440 (2021).
[19] P. Tang (unpublished).
[20] Y. Tserkovnyak, A. Brataas, G. E. W. Bauer, B. I. Halperin, Nonlocal magnetization dynamics in ferromagnetic heterostructures, Rev. Mod. Phys. **77**, 1375 (2005).
[21] L. Caretta, M. Mann, F. Büttner, K. Ueda, B. Pfau, C. M. Günther, P. Hessing, A. Churikova, C. Klose, M. Schneider, D. Engel, C. Marcus, D. Bono, K. Bagschik, S. Eisebitt, and G. S. D. Beach, Fast current-driven domain walls and small skyrmions in a compensated ferrimagnet, Nature Nanotechnol. **13**, 1154 (2018).
[22] L. Soumah, N. Beaulieu, L. Qassym, C. Carrétéro, E. Jacquet, R. Lebourgeois, J. B. Youssef, P. Bortolotti, V. Cros, and A. Anane, Ultra-low damping insulating magnetic thin films get perpendicular, Nature Commun. **9**, 3355 (2018).
[23] L. Alahmed and P. Li, Chapter 3 in: *Magnetic Materials and Magnetic Levitation*, edited by D. R. Sahu and V. N. Stavrou (IntechOpen Limited, London, 2021).
[24] B. Huang, G. Clark, E. Navarro-Moratalla *et al.*, Layer-dependent ferromagnetism in a van der Waals crystal down to the monolayer limit, Nature (London) **546**, 270 (2017).
[25] C. Koerner, R. Dreyer, M. Wagener, N. Liebing, H. G. Bauer, and G. Woltersdorf, Frequency multiplication by collective nanoscale spin-wave dynamics, Science **375**, 1165 (2022).
[26] G. Lan, K. Liu, Z. Wang, F. Xia, H. Xu, T. Guo, Y. Zhang, B. He, J. Li, C. Wan, G. E. W. Bauer, P. Yan, G. Liu, X. Pan, X. Han, and G. Yu (unpublished).
[27] L. Sheng, M. Elyasi, J. Chen, W. He, Y. Wang, H. Wang, H. Feng, Y. Zhang, I. Medlej, S. Liu, W. Jiang, X. Han, D. Yu, J.-P. Ansermet, G. E. W. Bauer, and H. Yu, Nonlocal Detection of Interlayer Three-Magnon Coupling, Phys. Rev. Lett. **130**, 046701 (2023).